Progress In Electromagnetics Research, Vol. 147, 37–56, 2014

Multiple Time Scales Optical Nonlinearities of Liquid Crystals for Optical-Terahertz-Microwave Applications

Iam Choon Khoo* **and Shuo Zhao**

(*Invited Review*)

Abstract—We provide a critical account of the dynamics of laser induced refractive index changing mechanisms in nematic liquid crystals which may be useful for all-optical switching and modulation applications in the visible as well as the Terahertz and long-wavelength regime. In particular, the magnitude and response times of optical Kerr effects associated with director axis reorientation, thermal and order parameter changes, coupled flow-reorientation effects and individual molecular electronic responses are thoroughly investigated and documented, along with exemplary experimental demonstrations. Emphases are placed on identifying parameter sets that will enable all-optical switching with much faster response times compared to their conventional electro-optics counterparts.

1. INTRODUCTIONS — LIQUID CRYSTALS FOR PHOTONIC AND ELECTROMAGNETIC APPLICATIONS

Liquid crystals (LC) are truly a special gift from nature, possessing dual fluid-crystalline properties and a whole slew of unique physical properties that are finding an ever increasing use in ubiquitous photonics devices [1–5] for information/image display, communication and processing applications. The most widely investigated ones are thermotropic liquid crystals which exhibit various ordered phases as a function of temperature. Figures 1(a)–(c) depict three commonly occurring phases: Smectic, Nematic and Cholesteric (chiral-Nematic).

In these ordered phases, the molecules are aligned in a general direction defined by a unit vector $\tilde{n}$, the so-called "director" axis. In Smectic phase, the molecules possess directional as well as position order; Smectic A phase, for example, exhibits layered structures. Nematic liquid crystals (NLC) molecules exhibit directional order, but are otherwise randomly positioned with fluidic properties. Bulk NLC's are generally centro-symmetric; their physical properties are the same in the $+\hat{n}$ and $-\hat{n}$ directions. Cholesteric liquid crystals (CLC) are formed by introducing chiral agents to the NLC molecular constituents during synthesis. The director axis of CLC spirals around an axis with a pitch that can be changed by adjusting the mixture concentration or temperature. As a result of the 1-D spatially periodic variation in the dielectric constant, the dispersion $\omega(\mathbf{k})$ exhibits energy bandgap and other 1-D photonic crystal properties [3].

This review is focused on nematic liquid crystals (NLC), which have now been incorporated in a wide assortment of active devices throughout the optical-Terahertz-microwave spectrum [1–46]. In this phase, the material exhibits dual fluid-crystalline properties, and has to be contained in some 'cell' or enclosure. The inner boundary surfaces of these structures are treated with an alignment layer to anchor the director axis in a desired orientation forming the equivalence of a crystalline axis. Conventional NLC-based electro-optical devices are usually assembled in planar configuration such as display screens [1]

Received 23 March 2014, Accepted 10 May 2014, Scheduled 20 May 2014
* Corresponding author: Iam Choon Khoo (ick1@psu.edu).
The authors are with the Department of Electrical Engineering, Pennsylvania State University, University Park, PA 16802, USA.

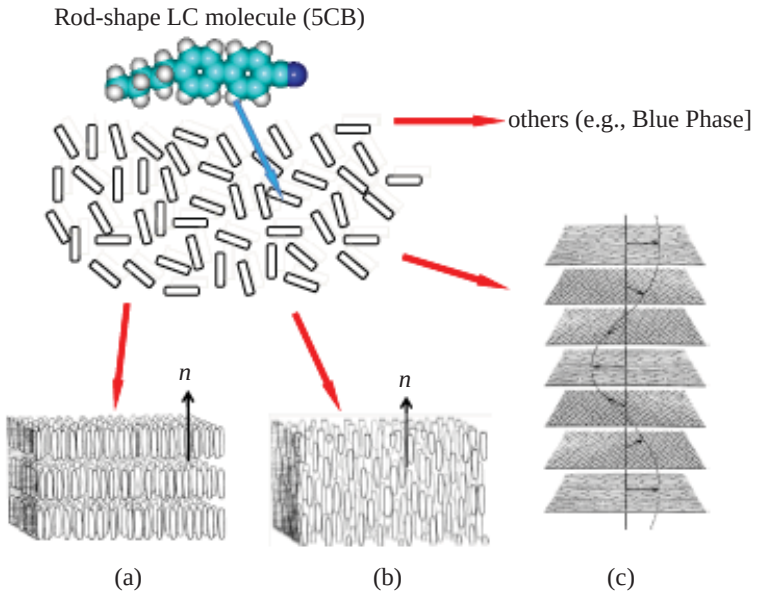

Figure 1. Spatial arrangement of the director axis $\tilde{n}$ in three commonly occurring phases of liquid crystals: smectic, nematic and chiral nematic (often termed cholesteric) liquid crystals. (a) Smectic A. (b) Nematic. (c) Cholesteric.

in the visible spectrum or metallic plates used for microwave operations [36], c.f. Figures 2(a)–(b). The fluid nature of NLC's and their compatibility with other widely used materials ranging from semiconductors to polymers and plasmonics (metals) enable easy integration of such 'crystal' into a large assortment of non-planar structures ranging from *nm-sized photonics elements* [7–25] such as inverse opal photonic crystals and plasmonic/metamaterial structures, c.f. Figures 2(c)–(d), to *millimeter- or bulkier microwave devices* for tunable — delay line, — phase shifter, — wavelength selector and beam steering devices [26–40], to name a few.

Nematic liquid crystals are uni-axial, characterized by refractive indices $n_{\|}$ and the $n_{\perp}$, for light polarization parallel and orthogonal to the director axis, respectively. The magnitude of nematic birefringence $\Delta n = n_{\|} - n_{\perp}$ is among the largest of all known materials, on the order of 0.2 that holds from the visible through far infrared and well into the microwave regime [1–3, 41–48], c.f. Figure 3 and Table 1. NLC with birefringence approaching unity in the visible regime are now routinely being produced [47, 48], and there are increasing efforts to synthesize NLC with large birefringence and low loss in the Terahertz and longer wavelength regime [41–46] paralleling the growth in interests in developing tunable electromagnetic devices.

The enormous magnitude of the birefringence means that an interaction length of a few wavelengths can impart a phase shift $\Delta\phi = 2\pi(\Delta n)d/\lambda$ of over 2π between the extraordinary and ordinary component of an optical or electromagnetic waves traversing the cell. More importantly, the birefringence can be easily modulated or controlled. For such purposes, the most widely exploited mechanism is field induced director axis reorientation, which results in a change in the refractive index. Most liquid crystals based devices such as the ubiquitous display screens in cell phones, TV and computer screens employ AC electric field, where the typical field needed to create reorientation is on the order of 1 volt/μm.

In this review, we provide a comprehensive account of the optical counterpart operations where changes in the birefringence or refractive index are produced by the optical electric field of lasers. In particular, we will investigate all the major mechanisms leading to the so-called optical Kerr effect [49] where the laser induced refractive index change is of the form: $\Delta n = n_2 I$ [I is the optical intensity and n_2 is the nonlinear index coefficient]. As detailed in the following sections, nonlinear index coefficients characterizing these nonlinear optical processes are among the largest of all known materials, ranging from $\sim 10^{-11}$ cm^2/Watt for ultrafast individual molecular electronic nonlinearities to well over 10^3 cm^2/W for liquid crystalline ordered phase nonlinearities [2–5, 40–78]. In contrast to

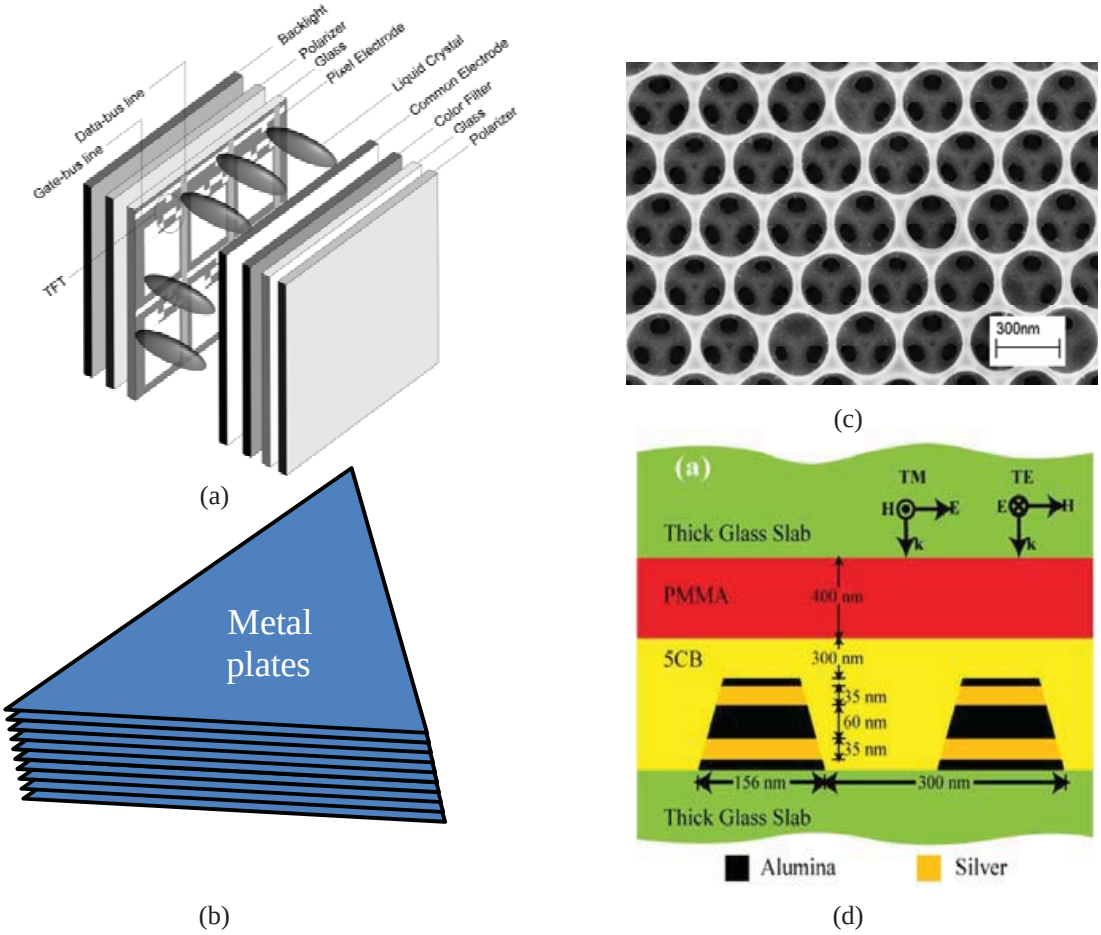

Figure 2. Nematic liquid crystal in photonics and microwave-structures. (a) Exploded view of a pixel element in typical LC display screen [2]. (b) Metallic stacks with interspersed NLC for millimeter wave beam manipulation [36]. (c) Nematic liquid crystal in inverse opal photonic crystal [8]. (d) Nematic liquid crystals in nanostructured metamaterial [12].

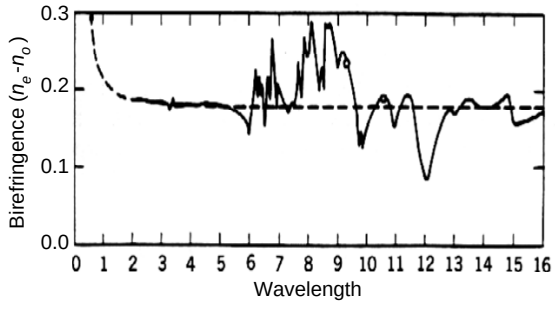

Figure 3. Birefringence of some typical nematic liquid crystals in the visible-infrared spectral region.

their electro-optical counterparts that operate at milliseconds speed, several of these optically activated mechanisms can enable ultrafast all-optical switching operations in conjunction with sub-microseconds to nanoseconds and femtoseconds lasers [65–84]. All-optical interactions and activation processes also do not require electrodes or complex circuitry, and can be mediated with a large degree of freedom in the direction and polarization states of the incident electromagnetic waves.

Table 1. Anisotropic physical parameters of a typical nematic liquid crystal (E7).

E7	$n_\parallel$	$n_\perp$	Δn	$\alpha_\parallel$ (cm^{-1})	$\alpha_\perp$ (cm^{-1})	**Spectral Region**
	1.75	1.525	0225	...	...	[$\lambda = 0.589\,\mu$m]
	1.71	1.50	0.21	...	...	[$\lambda = 1.55\,\mu$m]
	1.70	1.49	0.21	55	40	[$\lambda = 10.59\,\mu$m]
	1.73	1.57	0.16	0.9	3.1	[0.2 THz]
	1.76	1.62	0.14	7	27	[2 THz]
	$\varepsilon_\parallel = 3.25$	$\varepsilon_\perp = 2.78$	$\Delta\varepsilon = 0.47$			[60 GHz]

Thermal Diffusion constants [D=$\lambda_T/\rho_0 C_v$]

$$D_\parallel = 1.95 \times 10^{-3}\,\mathrm{cm}^2/\mathrm{s} \quad D_\perp = 1.2 \times 10^{-3}\,\mathrm{cm}^2/\mathrm{s}$$

Elastic constants:

$$K_1 = 1.2 \times 10^{-11}\,\mathrm{N};\ K_2 = 9 \times 10^{-12}\,\mathrm{N};\ K_3 = 1.95 \times 10^{-11}\,\mathrm{N}$$

Viscosity coefficients: at 20°C

γ_1 (Rotational Viscosity) = 283 mPa·s

η (Splay Viscosity) = 41 mm^2/s at 20°C; η (Twist Viscosity) = 37 mm^2/s at 20°C

2. MECHANISMS AND DYNAMICS OF LASER INDUCED REFRACTIVE INDEX OR BIREFRINGENCE CHANGES IN LIQUID CRYSTALS

Most NLC-based devices utilize the birefringence in combination with linearly polarized light which propagates as an extraordinary wave in the NLC cell, c.f. Figure 4, and experiences a θ-dependent refractive index $n_e(\theta)$ given by:

$$n_e^2(\theta) = \frac{n_\parallel^2 n_\perp^2}{n_\parallel^2 \cos^2(\theta) + n_\perp^2 \sin^2(\theta)} \tag{1}$$

The refractive indices $n_\parallel$ and $n_\perp$ of NLC are dependent on various molecular parameters and the

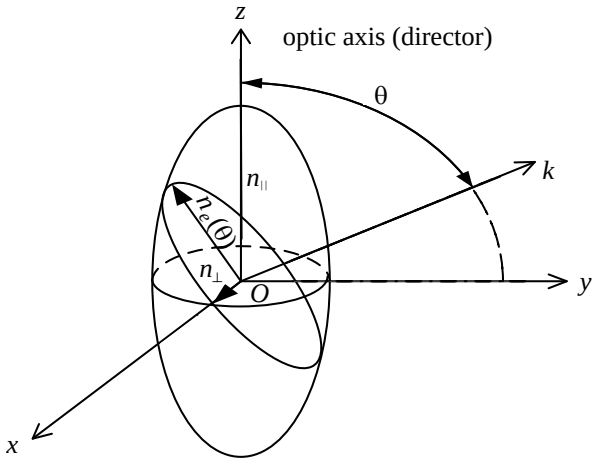

Figure 4. Index ellipsoid for extraordinary and ordinary waves propagating in a NLC with the director axis aligned in the z-direction.

order parameter S [2]:

$$n_{\|}^2 = \varepsilon_{\|} = 1 + \left(\frac{N}{3\varepsilon_0}\right)[\alpha_l K_l(2S+1) + \alpha_t K_t(2-2S) \tag{2}$$

$$n_{\perp}^2 = \varepsilon_{\perp} = 1 + \left(\frac{N}{3\varepsilon_0}\right)[\alpha_l K_l(1-S) + \alpha_t K_t(2+S) \tag{3}$$

$$\Delta\varepsilon = \left(\frac{N}{3\varepsilon_0}\right)[\alpha_l K_l - \alpha_t K_t]\, S \propto \frac{N_A \rho}{\varepsilon_0 M}(\alpha_l K_l - \alpha_t K_t)\, S \propto \rho S \tag{4}$$

Here (α_l, K_l) and (α_t, K_t are the values of the components of molecular polarizability and local field correction tensor $\vec{\vec{K}}$ parallel and perpendicular to the principal axis, respectively; N_A is the Avogadro number, M the molecular weight, and ρ the density [1–3]. S is the magnitude of the order parameter tensor $S_{\alpha\beta} = S(T)[n_\alpha n_\beta - \delta_{\alpha\beta}/3]$, where n_α and n_β are the spatial components of the director axis unit vector. The order parameter is highly dependent on the temperature, e.g., $S(T) = (1 - \frac{0.98TV^2}{T_c V_c^2})^{0.22}$ where V and V_c, are the molar volumes at T and T_c, respectively, T_c, being the nematic $\rightarrow$ isotropic phase transition temperature; other factor such as the presence of azo-dopant molecules, cell thickness and anchoring conditions, applied fields can also modify the order parameter and therefore the refractive indices.

An optical field, therefore, can create index or birefringence changes by changing the temperature, density, or the order parameters; NLC under intense short pulses have also been shown to exhibit flow-reorientation effects [4, 5, 66–69]. For clarity, we have arbitrarily divided the mechanisms into two classes — one pertaining to non-absorptive NLC, and the other to absorptive (with or without dopants) NLC. In the next few sections, we shall discuss the fundamentals of these mechanisms and their dynamical characteristics, and explore the possibilities of utilizing them for fast responding all-optical switching and modulation operations. For completeness and possibly new applications, we also include a brief discussion of the ultrafast (femtoseconds) molecular electronic nonlinearities [49, 77–85] of NLC, as well as the isotropic (liquid) phase nanoseconds orientation nonlinearities [3, 52, 53].

2.1. Laser Induced Director Axis Reorientation Nonlinearity in Transparent Nematic Liquid Crystals — Magnitude and Response Times

Consider an exemplary interaction configuration as shown in Figure 5 involving the application of various AC and optical fields on a homeotropically aligned NLC, where the director axis is aligned perpendicular to the cell boundaries. The applied fields could create one or more of the splay-, twist- and bend-types of lattice distortions, as well as fluidic flows with velocity v, as shown in Figure 6.

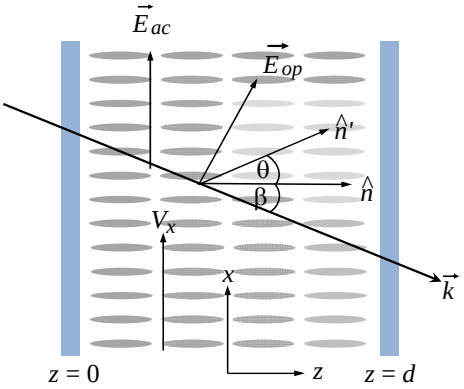

Figure 5. Schematic depiction of the interaction geometry involving AC and optical electric fields causing director axis reorientation and material flows in an aligned NLC cell.

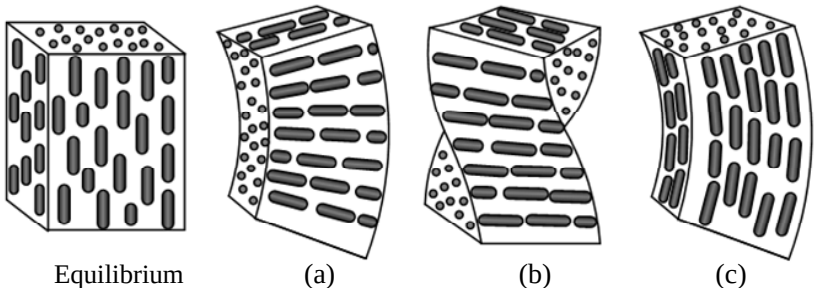

Figure 6. Nematic liquid crystal in their unperturbed state (e.g., homeotropic alignment) and field induced distortions: (a) splay, (b) twist, and (c) bend distortions that give rise to index and birefringence changes.

Field induced director axis reorientation is described by the continuum theory [1–3] which begins with the Free energies associated with the resulting distortions:

$$\text{Splay: } f_1 = \frac{1}{2}K_1\left(\nabla\cdot\hat{n}\right)^2; \quad \text{Twist: } f_2 = \frac{1}{2}K_2\left(\hat{n}\cdot\nabla\times\hat{n}\right)^2; \quad \text{Bend: } f_3 = \frac{1}{2}K_3\left(\hat{n}\times\nabla\times\hat{n}\right)^2 \tag{5}$$

Dielectric interactions between the applied fields [optical, AC] and the NLC's give rise to the corresponding Free energies: $f_{op} = -\Delta\varepsilon_{op}E_{op}^2$ and $f_{ac} = -\Delta\varepsilon_{ac}E_{ac}^2$, where $\Delta\varepsilon_{ac}$ and $\Delta\varepsilon_{op}$ are the AC and optical frequency dielectric anisotropies of NLC, respectively. *The dynamical* equation of motion describing the field induced director axis reorientation and flow is described by an Euler equation derived by minimization of the total Free energy of the systems $F_{total} = f_1 + f_2 + f_3 + f_{op} + f_{ac}$. For example, for the typical interaction geometry depicted in Figure 5, the dynamical equation becomes [2, 3]:

$$\begin{aligned}\gamma_1\frac{d\theta}{dt} = {} & \left[K_1\sin^2\theta + K_3\cos^2\theta\right]\frac{d^2\theta}{dz^2} + \left[(K_1-K_3)\sin\theta\cos\theta\right]\left(\frac{d\theta}{dz}\right)^2 + \left[\alpha_2\sin^2\theta - \alpha_3\cos^2\theta\right]\frac{dv}{dz} \\ & + \varepsilon o\varepsilon_{ac}E_{ac}^2\sin\left(\beta+\theta\right)\cos(\beta+\theta) + \varepsilon_o\Delta\varepsilon_{op}E_{op}^2 f(\beta,\theta)\end{aligned} \tag{6}$$

In Equation (6), α's and γ are various viscosity coefficients, K's the elastic constants. The spatial function $f(\beta, \theta)$ depends on the interaction geometry between the optical electric field polarization states and the angle of incidence.

Without loss of physics, consider the exemplary case involving director axis reorientation by *a polarized plane wave*. Ignoring flow and using the one elastic constant approximation ($K_1 = K_3 = K$), the dynamical torque balance equation becomes:

$$\gamma_1\frac{d\theta}{dt} = K\frac{d^2\theta}{dz^2} + \varepsilon_o\Delta\varepsilon E_{op}^2\sin 2(\beta+\theta) \tag{7}$$

In the steady-state ($d\theta/dt = 0$) and the usual case of small reorientation angle $\theta \ll 1$ and β, the solution for θ subject to the boundary conditions that $\theta = 0$ at $z = 0$ and at $z = d$ is given by:

$$\theta \sim \sin(2\beta)\left(dz - z^2\right)\varepsilon_o\Delta\varepsilon E^2/K \tag{8}$$

This gives rise to a *z-dependent refractive index change:*

$$\Delta n = n\left(\beta+\theta\right) - n\left(\beta+\theta\right) = \frac{n_\perp\Delta\varepsilon}{\varepsilon_\parallel n_\parallel}\left(\sin 2\beta\right)\theta = \alpha_2\left(z\right)I \tag{9}$$

Here I is the optical intensity ($I = n_\parallel E^2/2\eta$, where η is the free space impedance), and the local nonlinearity $\alpha_2(z)$ is given by:

$$\alpha_2 \sim \frac{2\varepsilon_0 n_\perp\Delta\varepsilon^2\eta}{\varepsilon_\parallel n_\parallel^2 K}\left(\sin 2\beta\right)^2\left(dz - z^2\right) \tag{10}$$

The local nonlinearity can be integrated and averaged over the cell thickness to give a measure of the nonlinear index coefficient n_2 of NLC cell as a whole:

$$n_2 = \langle \alpha_2 \rangle \sim \frac{\eta \varepsilon_0 n_\perp \Delta\varepsilon^2}{3\varepsilon_\parallel n_\parallel^2 K} (\sin 2\beta)^2 \, d^2 \tag{11}$$

Using typical nematic parameters [$\Delta\varepsilon = 0.64\varepsilon_o$; $\varepsilon_\parallel = 2.89\varepsilon_o$ ($\varepsilon_o = 8.85 \times 10^{-12}$ F/m); $K = 10^{-11}$ N] of a 50 µm thick cell ($d = 50$ µm), and assuming an incident internal angle $\beta = 22.5°$ in a 100 µm thick sample, i.e., $2\beta = 45$ degrees to maximize n_2, we get:

$$n_2 \sim 1 \times 10^{-4} \, \text{cm}^2/\text{W} \tag{12}$$

Compared to the laser induced orientation nonlinearity of the liquid phase counterpart or anisotropic liquid like CS_2 [49], the orientation nonlinearity of NLC is more than a million times larger.

The enormity of the orientation nonlinearity, nevertheless, is accompanied by a rather slow relaxation time. From the dynamical torque balance Equation (7), one can deduce a typical field-free director axis relaxation time:

$$\tau_\theta = \frac{\gamma_1 d^2}{K\pi^2} \tag{13}$$

If the cell thickness $d = 50$ µm, and $\gamma_1 = 0.1$ P, $K_1 = 10^{-11}$ N, the orientation relaxation time $\tau_\theta \approx 2.5$ s. Note that the response time is quadratically dependent on the cell thickness. For the usual cell gap of 5 µm used in display devices, $\tau_\theta = 25$ ms.

2.1.1. Ultrafast Director Axis Reorientation by Intense Short Pulses

Although the field-free director axis relaxation process is slow, the dynamics of the field induced reorientation process is controlled by the applied field strength, as one can see from Equation (7). In many applications where only one-way switching by the optical field is needed, the response time [defined by the time it takes to create sufficient reorientation and therefore sufficient phase-shift or index change to trigger the optical effect] could be sped up simply by increasing the optical field/intensity strength. This can be seen from the following simple consideration.

From (7), in the limit where $\theta \ll \beta$, we have:

$$\gamma_1 \frac{d\theta}{dt} = K \frac{d^2\theta}{dz^2} + \varepsilon_o \Delta\varepsilon E_{op}^2 \sin 2\beta \tag{14}$$

Consider an incident laser that is a flat top square pulse as shown in Figure 7: $E_{op}^2(t) = E_{op}^2$ for $0 < t < \tau_p$; $E_{op}^2(t) = 0$ otherwise. For a plane wave and again assuming hard boundary conditions, i.e., we can write $\theta = \theta(t)\sin(\pi z/d)$, the solution for $\theta(t)$ is:

$$\theta\,(t) = \tau_\theta \varepsilon_0 \Delta\varepsilon \mathrm{E}_{op}^2 \,(\sin 2\beta) \left(1 - e^{-t/\tau_\theta}\right) \tag{15}$$

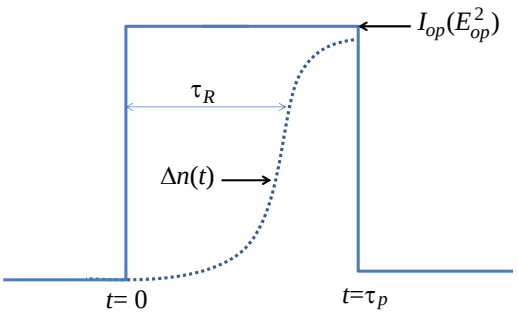

Figure 7. Transient induced refractive index change in response to a flat-top laser pulse.

For short pulses ($\tau_p \ll \tau_\theta$), we have therefore:

$$\theta\left(t\right) \sim \left(\tau_\theta/\gamma_1\right) \varepsilon_0 \Delta\varepsilon \mathrm{E}_{op}^2 \left(\sin 2\beta\right) \cdot t/\tau_\theta \tag{16}$$

Comparing $\theta(t)$ above with the steady state the maximum orientation (at $z = d/2$) from (9), we thus have:

$$\theta\left(t\right)/\theta^{ss} \sim \left(\frac{4}{\pi^2}\right)\left(t/\tau_\theta\right) \sim \left(t/\tau_\theta\right) \tag{17}$$

In (17) one may ignore the $(\frac{4}{\pi^2})$ factor as it arises from the different assumed z-dependence of θ in solving for the steady state and the dynamical equations. In the transient regime, therefore, the index change $\Delta n(t)$ induced by a pulse laser is of the form:

$$\Delta n(t) \sim (t/\tau_\theta)\Delta n^{ss} \tag{18}$$

One can thus define an *effective nonlinear index coefficient* $n_2^{\mathit{eff}}(\tau_{int})$ for short pulses that depends on the time of laser-material interaction τ_{int}:

$$n_2^{\mathit{eff}}(\theta, \tau_{in}) \sim (\tau_{int}/\tau_\theta) n_2 \tag{19}$$

For switching or modulation applications, it is clear that as soon as $\Delta n(t)$, or the phase shift $\delta\phi = \Delta n 2\pi d/\lambda$ [d = interaction length and λ = wavelength of light] reaches the required threshold, the optical switching/modulation process can be accomplished. The time it takes for the phase shift to reach the device operating requirement (e.g., $\delta\phi = \pi$) may be used to define a '**response time**' τ_R which is clearly inversely proportional to the laser intensity,

$$\tau_R(\theta) \propto 1/I_{op} \tag{20}$$

In other words, even though the free relaxation time constant may be in the milliseconds time scale, intense lasers with pulse duration of a few nanoseconds could induce sufficient director axis reorientation for nonlinear optical effects to manifest, as reported in [65–68]. The electro-optical analogue of such effect, i.e., fast onset of the director axis reorientation by a strong AC electric field has also been recently observed [86, 87]. The only but important caveat to this is that the effective nonlinearity is proportionally smaller for shorter interaction time, c.f. Equation (19), thereby requiring higher laser intensity to mediate the process.

2.1.2. Nanoseconds Laser Induced Flow-Reorientation Effect

In transparent NLC, coupled flow-reorientation effect [5, 66–69] caused by high intensity pulsed laser is another fast acting mechanism that can be used for all-optical switching. To determine the nonlinearity and dynamical characteristics of such process, probe beam diffraction from the index or polarization grating induced by optical wave mixing of two coherent nanoseconds lasers in the NLC is a frequently employed technique. For the interaction configuration employed in [68], the equations describing the coupled flow-reorientation process are given by:

$$\mu\frac{\partial^2\theta}{\partial t^2} + \gamma_1\frac{\partial\theta}{\partial t} - K\Delta\theta - \frac{1}{2}\left(\gamma_1 - \gamma_2 \mathrm{cos}2\theta\right)\frac{\partial v_x}{\partial y} = 0 \tag{21}$$

$$\rho_0\frac{\partial v_x}{\partial t} - \gamma_s\Delta v_x = F_x \tag{22}$$

Here θ is the director axis reorientation angle, v_x the velocity flow (in the x-direction), μ the moment of inertia, K the elastic constant, and γ_1, γ_2 and γ_3 are the viscosity coefficients. The driving force F_x in Equation (22) is the x-component of the Maxwell Stress: $F = (D\cdot\nabla)E^* - \frac{1}{2}\nabla(E\cdot D^*)$ exerted by the laser on the NLC and it is responsible for causing flows and director axis reorientation.

For the case where the input optical field is in the form of a polarization grating with amplitude $E(t)^2\cos(q_T y)$ where $q_T = 2\pi/\lambda_T$ with λ_T the grating constant, and assuming a step-on square pulse

of the form: $E^2(t) = 0$ for $t < 0$; $E^2(t) = E_o^2$ for $0 < t < \tau_p$, Equations (21) and (22) can be solved to yield a flow-reorientation $\theta = \theta_m(t)\cos(q_T y)$ with $\theta_m(t)$ given by [5, 69]:

$$\theta_m(t) = \frac{\varepsilon_0 E_0^2(\gamma_1 - \gamma_2)}{4\gamma_s K q_t^2}\left[1 - \frac{\tau_d e^{-t/\tau_d} - \tau_r e^{-t/\tau_r}}{\tau_d - \tau_r}\right] \tag{23}$$

$$\tau_d = \frac{\gamma_1}{K q_t^2}, \qquad \tau_r = \frac{\rho_0}{\gamma_s q_t^2} \tag{24}$$

Here τ_r measures the rise time of the flow-reorientation process. $\tau_r \sim 500$ nanoseconds for typical NLC parameters: $\rho_o \sim 10^3\,\mathrm{kg/m^3}$; $\gamma_s \sim 0.02\,\mathrm{kg/m{\cdot}s}$; $q_t \sim 3.18\,\mu\mathrm{m}^{-1}$ (grating constant of 20 µm); $\gamma_1 \sim 0.01\,\mathrm{kg/m{\cdot}s}$.

An important feature of this mechanism for director axis reorientation is that it is not dependent on the laser frequency, although it is highly dependent on the field/intensity gradients. As reported in [4, 5, 75] and briefly recapped in Section 2.2.3, this effect has been utilized for all-optical switching of pulsed lasers with response times in the microseconds to nanoseconds time scale.

2.1.3. Nanoseconds Laser Induced Electrostrictive Density Effect

Another mechanism that could be induced by a short intense laser pulse in transparent NLC is electrostriction — the movement of a dielectric material into region of high field strength [2, 3, 66–68]. In a typical grating diffraction set up used in [68], the induced density modulation created by a step-on flat top pulse is given by:

$$\rho^e(t) = \frac{\gamma^e E_0^2}{4\pi v^2}\left(1 - e^{-t/\tau_B}\cos\Omega t\right); \quad \tau_B = \frac{2\rho_0}{\eta q^2} \tag{25}$$

Here τ_B is the Brillouin relaxation constant (acoustic decay time) characterizing the propagating acoustic wave of frequency. $\Omega = \sqrt{q^2v^2 - \tau_B^{-2}}$ due to ρ^e. For typical NLC parameters: $\eta = 7 \times 10^{-2}\,\mathrm{kg\,m^{-1}s^{-1}}$, $\rho_0 = 10^3\,\mathrm{kg\,m^{-3}}$, and a grating period of 20 µm, $\tau_B \sim 200$ ns. Previous wave mixing [grating diffraction] studies with nanoseconds laser have shown that the interference between the oscillatory density component and the static thermal index grating created in the NLC gives rise to oscillations in the probe diffraction [67]; the magnitude of the density component is comparable (smaller by a factor of $\sim$4) to the transient thermal component discussed in Section 2.2.2.

2.1.4. Isotropic Phase Reorientation and Ultrafast Sub-picoseconds Laser Individual Molecular Electronics Nonlinearity

It is clear from the preceding discussions that the magnitude and response time of nonlinear index change of NLC form an inverse relationship, i.e., the larger is the nonlinearity, the longer is the response (or relaxation) time, i.e., n_2/τ_R is essentially a constant and is sometime used as a Figure of Merit (FOM). Thus, for director axis reorientation mechanism, the FOM is $\sim 10^{-4}/10^{-2} \sim 10^{-2}$. In this regards, the refractive index changing mechanism associated with laser induced ordering of isotropic (liquid) phase NLC is noteworthy as it yields comparable FOM; although the nonlinear index coefficient n_2 is smaller by a few orders of magnitude, the director axis relaxation time in the liquid phase is much shorter. From previous studies [52], the measured n_2 is on the order of $10^{-11}\,\mathrm{cm^2/Watt}$, while the response time is on the order of 10^{-9} s, i.e., FOM of isotropic NLC ($\sim 10^{-2}$) is comparable to the ordered phase. As the temperature of the liquid crystal is lowered towards the isotropic $\rightarrow$ nematic transition point (T_c), the nonlinearity increases but it is accompanied by a slowing down in the response speed [52]; nevertheless, the magnitude of the nonlinearity and the nanoseconds response time make this mechanism attractive for nonlinear optical application such as optical phase conjugation with nanosecond lasers [53].

At the individual molecular level, the dominant refractive index changing mechanism is laser induced complex third order nonlinear polarization whose real part effectively gives an intensity dependent refractive index, while the imaginary part is responsible for nonlinear absorptions [80–85]. Molecular electronic optical nonlinearities of bulk NLC are characterized by off-resonance n_2 values on the order of 10^{-14}–$10^{-13}\,\mathrm{cm^2/W}$, with sub-picoseconds response time ($\tau_R < 10^{-13}$ s) [2]. Recent studies of CLC (chiral nematic), which basically acts as a 1-D Bragg grating, have shown that because

of the grating feedback the nonlinearity can be enhanced by more than 2 orders of magnitude to give $n_2 \sim 10^{-12}$–10^{-11} for laser wavelength near the band edge of CLC [78]. Such unusually large fast responding electronic nonlinearity has been utilized for efficient direct compression of femtoseconds laser pulses with very thin (a few μm's) CLC cell [79].

2.2. Laser Induced Index Changing Mechanisms in Absorptive NLC — Enhanced Director Axis Reorientation, Thermal and Order-Parameter Effect

2.2.1. Enhanced Intermolecular Torque and Other Dopant Assisted Effects

In NLC containing photo-excitable dyes, another index changing mechanism is mediated by the intermolecular torque τ_{mole} exerted by the excited dye molecules on the surrounding NLC molecules. The magnitude of τ_{mole} can be over 2 orders of magnitude larger than the dielectric torque by the optical electric field τ_{op} that accounts for the driving term $\varepsilon_o \Delta\varepsilon E_{ac}^2 \sin 2(\beta+\theta)$ in the torque balance Equation (7) describing director axis reorientation, i.e., we have:

$$\tau_{mole} = \eta \tau_{op} \tag{26}$$

The sign of η depends on the particular dye dopants used [54–57], and its magnitude can be as large as over 10^2. Accordingly, the magnitude of the nonlinear index coefficients associated with this excited dye-molecules assisted director axis reorientation can be as large as $10^{-2}\,\mathrm{cm}^2/\mathrm{Watt}$, depending of course on the dye dopant concentration used. However, the response times of these dye dopant assisted reorientation are quite long, ranging from milliseconds to seconds in the nematic phase.

In NLC cells with a DC bias field, studies [58–62] have shown the possibility of similar enhanced response as a result of 'hetero-mixing' of the applied dc field with the optically generated space charge fields; n_2 values as high as $10^{-1}\,\mathrm{cm}^2/\mathrm{Watt}$ have been observed. In some dye-doped systems, surface alignment effects play an even more dominant role, leading to n_2 values $\gg 1\,\mathrm{cm}^2/\mathrm{Watt}$ [63, 64]. Nevertheless, the requirement of a strong DC bias [$> 1\,\mathrm{Volt}/\mu\mathrm{m}$], and the rather long response times make these effect unsuitable for practical switching applications.

2.2.2. Laser Induced Thermal and Order Parameter Changes

In absorbing NLC, or NLC's containing photo-excitable dopants, an impinging laser would create a temperature (ΔT) change that is described by the following equation [2, 3, 68]:

$$\rho_0 C_p \frac{\partial}{\partial t}(\Delta T) - \lambda_T \nabla^2 (T) = \alpha I_{op} \tag{27}$$

Here C_p is the specific heats, λ_T the thermal conductivity, ρ_0 the unperturbed density of the liquid crystal, α the absorption constant, and I_{op} the optical intensity. ΔT in turns gives rise to a change in the order parameter and consequently an index/birefringence change of the NLC. ΔT also produces density change, which is however much smaller in magnitude compared to the order parameter change, and could be neglected in most cases.

To estimate the magnitude and dynamics of the nonlinear index change associated with thermal effect, we again consider an NLC cell illuminated by an optical intensity grating of the form: $I(t) = I_o(t)\cos(\vec{q}\cdot\vec{y})$ where $I(t)$ is the intensity associated with a square flat-top laser pulse of duration τ_p. The temperature change ΔT is therefore of the form: $\Delta T = T(t)\cos(\vec{q}\cdot\vec{y})$ where $T(t)$ is the temperature grating amplitude

For $0 < t < \tau_p$, Equation (27) yields:

$$T(t) = \frac{\alpha I_{op}\tau_T}{\rho_0 C_v}\left(1 - e^{-t/\tau_T}\right); \quad \tau_T = \frac{\rho_0 C_v}{\lambda_T q^2} \tag{28}$$

For typical NLC parameters [2, 3]: $n \sim 1.5$, $\eta = 7\times 10^{-2}\,\mathrm{kg\,m^{-1}s^{-1}}$, $v = 1540\,\mathrm{m\,s^{-1}}$, $\rho_0 = 10^3\,\mathrm{kg\,m^{-3}}$, $\lambda_T/\rho_0 C_v = 0.79\times 10^{-7}\,\mathrm{m}^2/\mathrm{s}$, and a grating period of $20\,\mu\mathrm{m}$, the thermal decay time constant $\tau_T \approx 100\,\mu\mathrm{s}$.

In the steady state when the laser-NLC interaction time $\tau_p \gg \tau_T$, the temperature contribution builds up to a maximum value and produces an index change Δn_T given by:

$$\Delta n_T = \frac{\alpha I_{op} \tau_T}{\rho_0 C_v} \frac{dn}{dT} = n_2^{SS}(T)\, I_{op} \tag{29}$$

$$n_2^{SS}(T) = \frac{\alpha \tau_T}{\rho_0 C_v} \frac{dn}{dT} \tag{30}$$

For typical LC parameters: $C_v \approx 2\,\mathrm{J/g/K}$, $D \approx 2 \times 10^{-3}\,\mathrm{cm^2/s}$, $dn/dT \approx 10^{-3}\,\mathrm{K^{-1}}$ and assuming a grating period of 20 μm and $\alpha \sim 100\,\mathrm{cm^{-1}}$, we have:

$$n_2^{ss} \sim 2.5 \times 10^{-6}\,\mathrm{cm^2/W} \tag{31}$$

Near the nematic-isotropic transition temperature, the magnitude of the index gradient dn/dT (can be $dn_{\|}/dT$ or dn/dT *depending on the laser polarization*) and therefore the n_2 value can increase by almost two orders of magnitude [2, 51].

In photo-excitable NLC, another effective mechanism for order parameter change is Trans-Cis isomerism of azo-NLC or azo-molecule doped-NLC [71, 73, 76]. In the ground or unexcited state, the azo-molecule is in the Trans-state and conforms to the oblong shape of surrounding LC molecules. When photo-excited, the azo-molecule undergoes conformation changes to the Cis state and the resulting 'bent' shape creates local disorder, c.f. Figure 8, resulting in diminishing the NLC birefringence. Trans-Cis isomerism can occur very rapidly [e.g., picoseconds for Methyl-Red dye molecules], so the turn on time of the nonlinear optical process is dictated by how fast the surrounding LC order parameter can be perturbed; studies [71, 74, 76] have shown that the reaction time can be as short as a few nanoseconds.

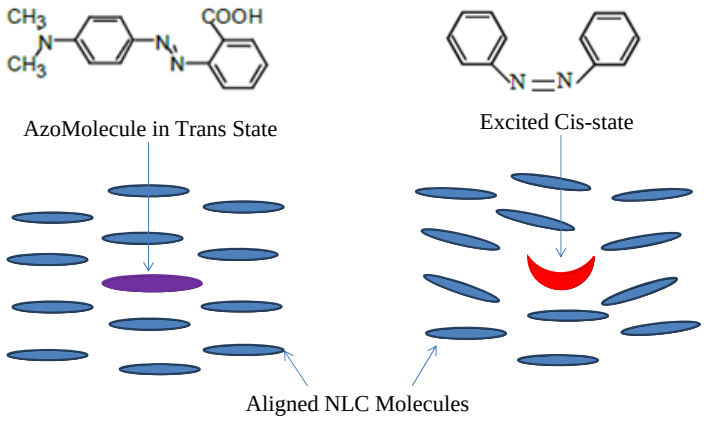

Figure 8. Schematic depiction of Azo-dopant undergoing Trans-Cis isomerism and perturb the order parameter of the aligned NLC host medium.

2.2.3. Laser Induced Thermal-Order Parameter Changes in NLC for Ultrafast Switching

In complete analogy to the case of transient laser induced director axis reorientation, c.f. the diffusive Equations (15) and (27), one can obtain similar fast switching effect with the use of short intense laser induced thermal effect. From Equations (29)–(31), the interaction-time-dependent effective nonlinear index coefficient is similarly given in the form:

$$n_2^{eff}(T, \tau_{in}) \sim (\tau_{int}/\tau_T) n_2^{SS}(T) \tag{32}$$

This shows that if the interaction time τ_{in} is 10^3 times shorter than τ_T, i.e., $\tau_{int} = 100\,\mathrm{ns}$, the effective n_2 value is $\sim 10^{-9}\,\mathrm{cm^2/W}$, which is in fact much larger than the director axis counterpart (which for similar interaction time yields a nonlinearity about two orders of magnitude smaller) and other mechanisms discussed so far [49]. Laser induced thermal/order parameter change in NLC, therefore, would enable very rapid and efficient one-way optical switching with relatively low threshold intensity requirements.

Perhaps the most illustrative NLC cell for all-optical switching is the 90° twist-aligned nematic cell [73] sandwiched between two crossed polarizers as shown in Figure 9. An incoming vertically polarized light would have its polarization vector rotated by the director axis's twist alignment to emerge from the cell with a horizontal polarization which is fully transmitted by the exit polarizer. By modulating the birefringence of the NLC, and therefore the polarization state of the light after traversing the NLC cell, one can modulate the transmission at the output end.

In electro-optics switching devices [1], an applied AC-field across the transparent electrode–coated cell walls would cause the director axis to realign normal to the cell walls, and thus the light remains vertically polarized in traversing the NLC and is extinguished at the output end. In all-optical switching, obviously there is no need for the transparent electrode coating as the birefringence change is induced by the laser through one or more of the self-action mechanisms discussed above; a low intensity pulse that causes insignificant birefringence change will be fully transmitted whereas a high intensity pulse will have its later portion switched off if sufficient birefringence change is induced by the initial portion of the pulse.

We have modeled the self-induced transmission switching effect of a Gaussian pulse of the form: $E^2 = E_0^2 e^{-t^2/\tau_p^2}$ propagating through a dye-doped NLC 90°-twist alignment cell using a Modified Jones Matrix method similar to those described in [73] for the set up as depicted in Figure 9. The mechanism employed in this simulation is the thermal effect, with the following parameters chosen to be close to experimental values. For the NLC, we have: absorption constant $\alpha = 100\,\mathrm{cm}^{-1}$, cell thickness = 200 μm, initial birefringence value $\Delta n = 0.16$ and a temperature index coefficient $dn/dT = 6 \times 10^{-2}/\mathrm{K}$ for sample initially at ∼3°K from Tc. The laser parameters used are: pulse duration: 250 ns; beam waist ω_o∼100 μm. Figure 10 shows the simulation results for the transmitted laser pulse for different input pulse energies. The plots show that for input laser pulse energy above ∼2.5 μJ, the later portion of the pulse exhibits obvious switching-off behavior. With increasing input laser energies, the switching-off process occurs earlier and earlier.

Using NLC doped with a variety of absorbing dyes, we have observed such self-action switching effects on various CW — pulsed lasers in the visible — near infrared spectrum. Figure 11 shows a typical observed switching behavior for input laser energy above a certain threshold. The dynamics of the transmitted pulse, the input pulse energy threshold to generate noticeable transmission switching are close to theoretical expectations. The switch-off occurs earlier for higher input lasers energies and response times as short as 50 nanoseconds have been observed [4, 5, 73–75].

Similar switching effects have been observed using transparent sample [4, 5, 75], where the mechanism involved is flow-orientation effect associated with Maxwell Stress described in Section 2.1.2. Typical input laser energy needed for the transmission to exhibit noticeable switching is much higher, on the order of 90 μJ. However, since the effect does not rely on absorbing dye-doping, it can be used in conjunction with focused lasers over a very wide spectrum spanning the visible to infrared and beyond.

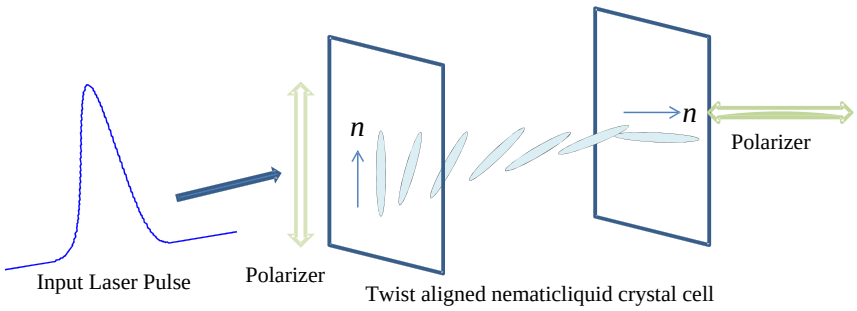

Figure 9. Typical optical transmission switching set up with a 90°-twist alignment NLC cell placed between two crossed polarizers for an initial clear state operation.

3. MULTIPLE TIME SCALES NONLINEARITIES OF NEMATIC LIQUID CRYSTALS — MERITS AND LIMITATIONS

From the preceding analyses, one can see that there is an apparent inverse relationship between the magnitude of the nonlinearity n_2 and the relaxation time constants τ. Mechanisms characterized by slow relaxation time produce larger nonlinearities, and vice versa. For example, ultrafast sub-picosecond individual molecular electronic nonlinearity is a few orders of magnitude smaller than the much slower macroscopic crystalline nonlinearities. In the ordered phase, this trend is best exemplified by the steady state orientation and thermal nonlinearities $-n_2$ in (11) and n_2^{ss} in (31), respectively since both processes are described by analogous diffusive equations. For the same NLC material parameters, the magnitude of n_2 and relaxation times τ of the nonlinearity is governed by the characteristic distortion or diffusion length involved. Thus, for $d = 50\,\mu\text{m}$, we have $n_2 = 1 \times 10^{-4}\,\text{cm}^2/\text{W}$ and τ (θ, $50\,\mu\text{m}$) $= 25\,\text{ms}$. One can get a faster response with a thinner sample, e.g., for $d = 20\,\mu\text{m}$, we have τ (θ, $20\,\mu\text{m}$)$\sim$4 ms but a proportionally smaller nonlinearity $n_2 = 1.6 \times 10^{-5}\,\text{cm}^2/\text{W}$. Similar analysis of Equations (30)–(32) yields the same inverse relationship between nonlinearity and relaxation time. For $d = 50\,\mu\text{m}$, we have n_2^{ss} (T, $50\,\mu\text{m}$) $\sim 1.6 \times 10^{-5}\,(\text{cm}^2/\text{W})$ and τ (T, $50\,\mu\text{m}$) $= 625\,\mu\text{s}$. On the other hand, for $d = 20\,\mu\text{m}$, we have τ (T, $20\,\mu\text{m}$) $= 100\,\mu\text{s}$ but then a proportionally smaller nonlinearity with n_2^{ss} (T, $20\,\mu\text{m}$) $\sim 2.5 \times 10^{-6}(\text{cm}^2/\text{W})$.

It is important to note that with the exception of individual molecular electronic nonlinear responses, the nonlinearities associated with all other mechanisms involve many material and optical parameters with wide ranging values, and it is not possible to ascribe a **definitive value** for n_2 or τ_{res} for each mechanism. For examples, both n_2 and τ_{res} for laser induced director axis reorientation as well as thermal effect in the ordered nematic phase can vary by many orders of magnitude depending on various factors such as cell dimension, interaction-geometry, absorption constant, dopant concentration/types, temperatures, and the spectral and temporal characteristics of the laser.

With these 'cautionary notes' in mind, we have depicted some exemplary 'data' points in Figure 12 for all the major mechanisms discussed in the preceding sections. The n_2 values quoted for a particular mechanism include their steady state (interaction time > free relaxation time), and their transient values (interaction time < free relaxation time) estimated using the same laser intensity used in the steady-state case. For dopant mediated mechanisms such as thermal, order parameter and photorefractive effects (where the presence of a dc bias field is another factor to contend), we show only representative

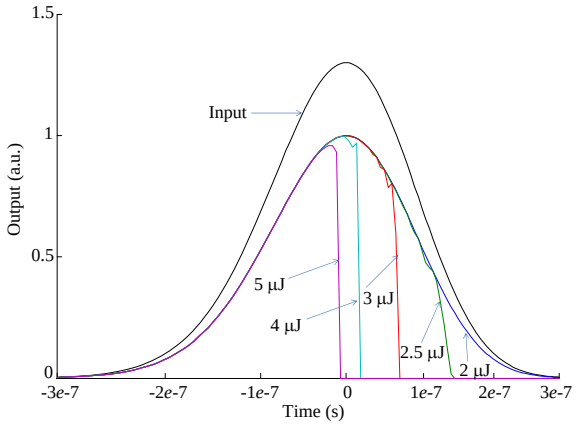

Figure 10. Theoretical simulation of the nonlinear transmission of a laser pulse through the 90°-twist alignment nematic liquid crystal cell using a modified Jone Matrix method [72].

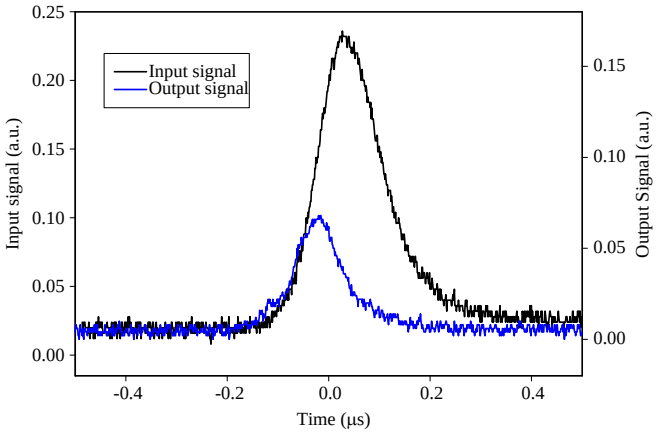

Figure 11. Oscilloscope traces of typical input (upper trace) and transmitted output laser pulse (lower trace) through a IR dye-doped 5CB sample Experimental parameters: laser wavelength: 750 nm; pulse duration: 250 ns; laser spot size: 140 μm; NLC thickness: 200 μm; input laser energy: 2 μJ [4].

values from the literature where the nonlinear optical responses were observed in samples of reasonable ($< 50\%$) absorption loss.

It is important to note here that we are NOT comparing the relative merits or 'performance characteristics' of different mechanisms, nor implying that these results depict some definitive general relationship between n_2 and τ. Rather, this plot is meant to provide a rough overview and a quick guide to selecting the appropriate mechanism for some specific application with desired response time and optical laser intensity/energy. For example, if one desire microseconds to nanoseconds response, thermal and order parameter modulation is arguably the most appropriate candidate. If absolute transparency or laser wavelength independence is mandated, then purely director axis reorientation, flow orientation or electrostriction should be considered. To make the final choice, the details for the chosen mechanisms can be obtained from the discussions in preceding sections and the quoted literatures.

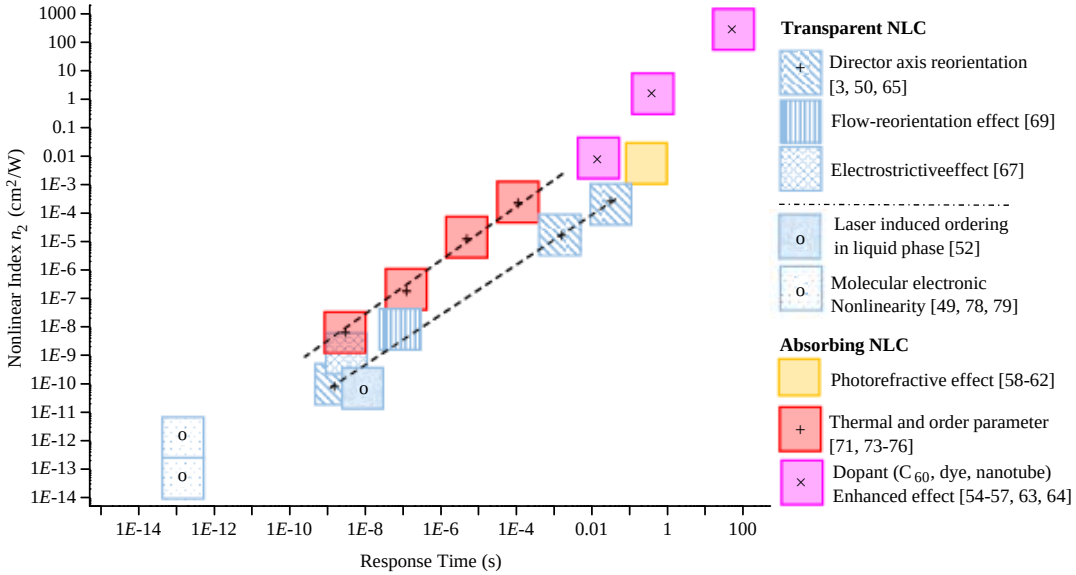

Figure 12. Exemplary values for steady-state and effective nonlinear index coefficients and response times of major mechanisms for laser induced refractive index modification of NLC.

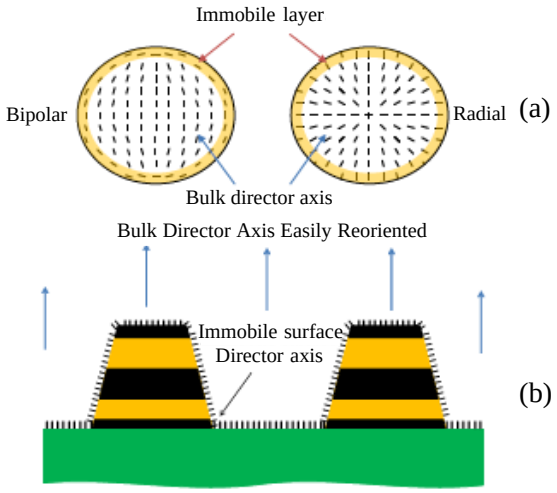

Figure 13. NLC director axis-distribution (a) inside a photonic crystal inverse opal [8] and (b) around the nanostructures of a negative permeability metamaterial [12].

With such multiple time scales optical nonlinearity and possessing many advantages over other materials, NLC are nevertheless beset with some inherent limitations. Generally speaking, their fluid nature demands encapsulation, which preclude them from many applications requiring free standing solid film/structure. Their polarization sensitivity naturally imposes rather restrictive conditions on complex structures designed for transformation optics or other operations associated with sub-unity or negative index [88–91], besides the obvious optical loss when used with un-polarized light or EM waves. The requirement of strong boundary surface anchoring/alignment to fabricate NLC cells invariably creates an immobile layer, c.f. Figure 13(a) that tends to diminish the overall response of the NLC-infiltrated structures such as inverse opal photonic crystal or micro-ring resonator [7, 11]. In complex non-planar structures with numerous tight corners and crevices such as fishnet or split-ring metamaterials other sub-wavelength structures and resonators [12–25] non-uniform director axis alignment, c.f. Figure 13(b) in addition to the immobile layer significantly diminish the effective tunable birefringence of the NLC and device performance.

Some of these limitations can be overcome by ingenious redesigning of the structures, use of dopants and/or more appropriate choice of mechanism. There have also been recent studies of another phase of chiral nematic liquid crystals, namely, Blue-Phase Liquid Crystals (BPLC) and their polymer-stabilized forms (PSBPLC) that presented promising polarization- and alignment-free alternatives [5, 92–99] for nonlinear optics as well as electro-optics. In this unique class of optical materials formed by mixing chiral and achiral nematics (with or without polymer stabilization), the molecules self-assemble into tightly wound defect-spirals that form 3-D cubic or BCC lattices with sub-wavelength lattice constants. They are therefore *optically isotropic*, i.e., respond to omni-directional light of any polarization state and yet possess optical nonlinearity of 'giant' magnitude comparable to nematics [92]. In addition, owing to the subdued director axis fluctuations of the tightly wound cholesteric spirals, scattering loss and relaxation times of BPLC's are greatly reduced. This allows high transmission through much longer path lengths [94] and the generation of large phase shift with much lower threshold power requirement and faster response times than typical nematics. Since BPLC constituents are organic molecules similar to NLC that possess large two-photon and excited state absorption efficiencies, they are also promising candidates for ultrafast (picosecond and femtosecond) nonlinear transmission, optical limiting and pulse compression operations.

4. CONCLUSION

In conclusion, we have presented a critical review of major index changing mechanisms in nematic liquid crystals that are capable of very fast response times compared to conventional NLC electro-optics and can be applied to devices operating in a very wide spectrum spanning the visible through Terahertz and into the microwave regime. The freedom from complex electronic circuitry, versatility and large degree of freedom in the use of optical fields, and the increasing availability of new high performance NLC (as well as BPLC) liquid crystalline systems tailored made for the spectral regime of interest make it all the more attractive to employ all-optical means to devise active photonics and electromagnetic devices.

ACKNOWLEDGMENT

This work is supported by the US Air Force Office of Scientific Research.

REFERENCES

1. Khoo, I. C. and S. T. Wu, *Optics and Nonlinear Optics of Liquid Crystals,* World Scientific, Singapore, 1994.
2. Khoo, I. C., *Liquid Crystals*, 2nd Edition, Wiley, NJ, 2007.
3. Khoo, I. C., "Nonlinear optics of liquid crystalline materials," *Physics Report*, Vol. 471, Nos. 5–6, 221–267, 2009.
4. Khoo, I. C., "Extreme nonlinear optics of nematic liquid crystals," *J. Opt. Soc. Am. B*, Vol. 28, A45–A55, 2011.

5. Khoo, I. C., "Nonlinear optics, active plasmonics and tunable metamaterials with liquid crystals," *Progress in Quantum Electronics*, Vol. 38, 77–117, 2014.
6. Sambles, J. R., R. Kelly, and R. F. Yang, "Metal slits and liquid crystals at microwave frequencies," *Philos. Transact. A, Math. Phys. Eng. Sci.*, Vol. 364, No. 1847, 2733–2746, 2006.
7. Khoo, I. C., Y. Z. Williams, A. Diaz, K. Chen, J. A. Bossard, L. Li, D. H. Werner, E. Graugnard, J. S. King, S. Jain, and C. J. Summers, "Liquid-crystals for tunable photonic crystals, frequency selective surfaces and negative index material development," *Mole. Cryst. Liq. Cryst.*, Vol. 453, 309–319, 2006.
8. Graugnard, E., J. S. King, S. Jain, C. J. Summers, Y. Zhang-Williams, and I. C. Khoo, "Electric field tuning of the Bragg peak in large-pore TiO_2 inverse shell opals," *Phys. Rev. B*, Vol. 72, 233105-1–233105-4, 2005..
9. D'Alessandro, A., R. Asquini, M. Trotta, G. Gilardi, R. Beccherelli, and I. C. Khoo, "All-optical intensity modulation of near infrared light in a liquid crystal channel waveguide," *Appl. Phys. Lett.*, Vol. 97, No. 9, 093302, 2010.
10. Larsen, T. T., A. Bjarklev, D. S. Hermann, and J. Broeng, "Optical devices based on liquid crystal photonic bandgap fibers," *Optics Express*, Vol. 11, 2589–2596, 2003.
11. Ptasinski, J., S. W. Kim, L. Pang, I.-C. Khoo, and Y. Fainman, "Optical tuning of silicon photonic structures with nematic liquid crystal claddings," *Optics Letters*, Vol. 38, 2008–2010, 2013.
12. Xiao, S., U. K. Chettiar, A. V. Kildishev, V. Drachev, I. C. Khoo, and V. M. Shalaev, "Tunable magnetic response of metamaterials," *Appl. Phys. Lett.*, Vol. 95, No. 3, 033115, 2009.
13. Minovich, A., J. Farnell, D. N. Neshev, I. McKerracher, F. Karouta, J. Tian, D. A. Powell, I. V. Shadrivov, H. H. Tan, C. Jagadish, and Y. S. Kivshar, "Liquid crystal based nonlinear fishnet metamaterials," *Appl. Phys. Lett.*, Vol. 100, 121113-4, 2012.
14. Zhao, Q., L. Kang, B. Du, B. Li, J. Zhou, H. Tang, X. Liang, and B. Z. Zhang, "Electrically tunable negative permeability metamaterials based on nematic liquid crystals," *Appl. Phys. Lett.*, Vol. 90, 011112, 2007, and References therein.
15. Zhang, F. L., W. H. Zhang, Q. Zhao, J. B. Sun, K. P. Qiu, J. Zhou, and D. Lippens, "Electrically controllable fishnet metamaterial based on nematic liquid crystal," *Optics Express*, Vol. 19, 1563–1568, 2011.
16. Bossard, J. A., X. Liang, L. Li, S. Yun, D. H. Werner, B. Weiner, T. S. Mayer, P. F. Cristman, A. Diaz, and I. C. Khoo, "Tunable frequency selective surfaces and negative-zero-positive index metamaterials based on liquid crystals," *IEEE Transactions on Antennas and Propagation*, Vol. 56, No. 5, 1308–1320, 2008.
17. Wang, X., D. H. Kwon, D. H. Werner, I. C. Khoo, A. Kildishev, and V. M. Shalaev, "Tunable optical negative-index metamaterials employing anisotropic liquid crystals," *Appl. Phys. Lett.*, Vol. 91, 143122, 2007.
18. Werner, D. H., D. H. Kwon, and I. C. Khoo, "Liquid crystal clad near-infrared metamaterials with tunable negative-zero-positive refractive indices," *Optics Express*, Vol. 15, 3342–3347, 2007.
19. Zhao, Y., Q. Z. Hao, Y. Ma, M. Q. Lu, B. X. Zhang, M. Lapsley, I. C. Khoo, and T. J. Huang, "Light-driven tunable dual band absorber with liquid-crystal-plasmonic asymmetric nanodisk array," *Appl. Phys. Lett.*, Vol. 100, 053119, 2012.
20. Huang, T. J., Y. J. Liu, B. Yue, J. Liou, and I. C. Khoo, "All-optical modulation of localized surface plasmon coupling in a hybrid system composed of photo-switchable gratings and Au nanodisk arrays," *Journal of Physical Chemistry*, Vol. 115, No. 15, 7717–7722, 2011.
21. Hao, Q., Y. Zhao, J. B. Krishna, I. C. Khoo, and T. Huang, "Frequency-addressed tunable transmission in optically thin metallic nanohole arrays with dual-frequency liquid crystals," *J. Appl. Phys.*, Vol. 109, 084340, 2011.
22. Liu, Y. J., Q. Z. Hao, J. S. T. Smalley, J. Liou, I. C. Khoo, and T. J. Huang, "A frequency-addressed plasmonic switch based on dual-frequency liquid crystals," *Appl. Phys. Lett.*, Vol. 97, 091101, 2010.

23. Dickson, W., G. A. Wurtz, P. R. Evans, R. J. Pollard, and A. V. Zayats, "Electronically controlled surface plasmon dispersion and optical transmission through metallic hole arrays using liquid crystal," *Nano Letts.*, Vol. 8, No. 1, 281–286, 2008.
24. Kossyrev, P. A., A. J. Yin, S. G. Cloutier, D. A. Cardimona, D. H. Huang, P. M. Alsing, and J. M. Xu, "Electric field tuning of plasmonic response of nanodot array in liquid crystal matrix," *Nano Letts.*, Vol. 5, 1978–1981, 2005.
25. Daly, K. R., S. Abbott, G. D'Alessandro, D. C. Smith, and M. Kaczmarek, "Theory of hybrid photorefractive plasmonic liquid crystal cells," *J. Opt. Soc. Am.*, Vol. 28, 1874–1881, 2011.
26. Hu, W., R. Cahill, J. A. Encinar, et al., "Design and measurement of reconfigurable millimeter wave reflectarray cells with nematic liquid crystal," *IEEE Transactions on Antennas and Propagation*, Vol. 56, No. 10, 3112–3117, 2008.
27. Kuki, T., H. Fujikake, and T. Nomoto, "Microwave variable delay line using dual-frequency switching-mode liquid crystal," *IEEE Trans. Microw. Theory Tech.*, Vol. 50, No. 11, 2604–2609, 2002.
28. Dolfi, D., M. Labeyrie, P. Joffre, and J. P. Huignard, "Liquid crystal microwave phase shifter," *Electron. Lett.*, Vol. 29, No. 10, 926–928, May 1993.
29. Kuki, T., H. Fujikake, T. Nomoto, and Y. Utsumi, "Design of a microwave variable delay line using liquid crystal and a study of its insertion loss," *Electron. Commun. Jpn.*, Vol. 85, No. 2, 36–42, Feb. 2002.
30. Kamei, T., Y. Utsumi, H. Moritake, K. Toda, and H. Suzuki, "Measurements of the dielectric properties of nematic liquid crystal at 10 kHz to 40 GHz and application to a variable delay line," *Electron. Commun. Jpn.*, Vol. 86, No. 8, 49–60, Aug. 2003.
31. Fujikake, H., T. Kuki, T. Nomoto, Y. Tsuchiya, and Y. Utsumi, "Thick polymer-stabilized liquid crystal films for microwave phase control," *J. Appl. Phys.*, Vol. 89, 5295–5298, 2001.
32. Guerin, F., J. M. Chappe, P. Joffre, and D. Dolfi, "Modelling, synthesis and characterization of a millimeter-wave multilayer microstrip liquid crystal phase shifter," *Jpn. J. Appl. Phys.*, Vol. 36, 4409–4413, 1997.
33. Hibbins, A. P., J. R. Sambles, C. R. Lawrence, and D. M. Robinson, "Remarkable transmission of microwaves through a wall of metallic bricks," *Appl. Phys. Lett.*, Vol. 79, 2844–2846, 2001.
34. Lim, K. C., J. D. Margerum, and A. M. Lackner, "Liquid crystal millimetre wave electronic phase shifter," *Appl. Phys. Lett.*, Vol. 69, 1065–1067, 1993.
35. Lim, K. C., J. D. Margerum, A. M. Lackner, L. J. Miller, E. Sherman, and W. H. Smith, "Liquid crystal birefringence for millimetre wave radar, *Liq. Cryst.*, Vol. 14, 327–337, 1993.
36. Tanaka, M. and S. Sato, "Millimetre-wave deflection properties of liquid crystal prism cells with stack-layered structure, *J. Appl. Phys.*, Vol. 40, L1123–L1125, 2002.
37. Tanaka, M. and S. Sato, "Focusing properties of liquid crystal lens cells with stack-layered structure in the millimetre wave region," *IEEE Microw. Wireless Component Lett.*, Vol. 12, 163–165, 2002.
38. Kowerdzieja, R., J. Parka, and J. Krupkab, "Experimental study of thermally controlled metamaterial containing a liquid crystal layer at microwave frequencies," *Liq. Cryst.*, Vol. 38, 743–747, 2011.
39. Yang, F. and J. R. Sambles, "Microwave liquid crystal wavelength selector," *Appl. Phys. Lett.*, Vol. 79, 3717–3719, 2001.
40. Yang, F. and J. R. Sambles, "Microwave liquid crystal variable phase grating," *Appl. Phys. Lett.*, Vol. 85, 2041–2043, 2004.
41. Li, J., S. T. Wu, S. Brugioni, R. Meucci, and S. Faetti, "Infrared refractive indices of liquid crystals," *J. Appl. Phys.*, Vol. 97, No. 7, 073501–073501, 2005.
42. Yang, C. S., C. J. Lin, R. P. Pan, C. T. Que, K. Yamamoto, M. Tani, and C. L. Pan, "The complex refractive indices of the liquid crystal mixture E7 in the terahertz frequency range," *J. Opt. Soc. Am. B*, Vol. 27, No. 4, 1866–1873, 2010.
43. Park, H., E. P. J. Parrott, F. Fan, M. Lim, H. Han, V. G. Chigrinov, and E. Pickwell-MacPherson, "Evaluating liquid crystal properties for use in terahertz devices," *Optics Express*, Vol. 20, 11899–

11905, 2012.

44. Wang, L., X.-W. Lin, X. Liang, J.-B. Wu, W. Hu, Z.-G. Zheng, B.-B. Jin, Y.-Q. Qin, and Y.-Q. Lu, "Large birefringence liquid crystal material in terahertz range," *Opt. Mat. Exp.*, Vol. 2, 1314–1319, 2012.
45. Weil, C., S. Mueller, P. Scheele, P. Best, G. Lüssem, and R. Jakoby, "Highly-anisotropic liquid-crystal mixtures for tunable microwave devices," *Electron. Lett.*, Vol. 39, No. 24, 1732–1734, Nov. 2003.
46. Mueller, S., A. Penirschke, C. Damm, P. Scheele, M. Wittek, C. Weil, and R. Jakoby, "Broad-band microwave characterization of liquid crystals using a temperature-controlled coaxial transmission line," *IEEE Trans. Microw. Theory Tech.*, Vol. 53, No. 6, 1937–1945, Jun. 2005.
47. Arakawa, Y., S. Nakajima, S. M. Kang, M. Shigeta, G. Konishi, and J. Watanabe, "Design of an extremely high birefringence nematic liquid crystal based on a dinaphthyl-diacetylene mesogen," *J. Mat. Chem.*, Vol. 22, 13908–13910, 2012, and References therein.
48. Okano, K., O. Tsutsumi, A. Shishido, and T. Ikeda, "Azotolane liquid-crystalline polymers: Huge change in birefringence by photoinduced alignment change," *J. Am. Chem. Soc.*, Vol. 128, 15368–15369, 2006.
49. Christodoulides, D. N., I. C. Khoo, G. J. Salamo, G. I. Stegeman, and E. W. Van Stryland, "Nonlinear refraction and absorption: Mechanisms and magnitudes," *Adv. Opt. Photon.*, Vol. 2, 60–200, 2010.
50. Khoo, I. C., "Re-examination of the theory and experimental results of optically induced molecular reorientation and nonlinear diffractions in nematic liquid crystals: Spatial frequency and temperature dependence," *Phys. Rev.*, Vol. 27, 2747–2750, 1983, and References therein.
51. Khoo, I. C. and R. Normandin, "The mechanism and dynamics of transient thermal grating diffraction in nematic liquid crystal films," *IEEE J. Quant. Electronics*, Vol. 21, No. 4, 329–335, 1985.
52. Khoo, I. C. and Y. R. Shen, "Liquid crystals-nonlinear optical properties and processes," *Opt. Eng.*, Vol. 24, 579–585, 1985.
53. Fekete, D., J. AuYeung, and A. Yariv, "Phase conjugation reflection by degenerate four wave mixing in a nematic crystal in the isotropic phase," *Optics Letters*, Vol. 5, 51–53, 1980.
54. Janossy, I. and T. Kosa, "Influence of anthraquinone dyes on optical reorientation of nematic liquid crystals," *Optics Letters*, Vol. 17, 1183–1185, 1992.
55. Li, H., Y. Liang, and I. C. Khoo, "Transient laser induced orthogonal director axis reorientation in dye-doped liquid crystal," *Mol. Cryst. Liq. Cryst.*, Vol. 251, 85–92, 1994.
56. Yang,P., L. Liu, L. Xu, and Y. R. Shen, "Excitation-enhanced optical reorientation in nematic liquid crystals," *Optics Letters*, Vol. 15, 2252–2254, 2009.
57. Khoo, I. C., H. Li, and Y. Liang, "Optically induced extraordinarily large negative orientational nonlinearity in dye-doped-liquid crystal," *IEEE J. Quant. Electronics*, Vol. 29, No. 5, 1444–1447, 1993.
58. Rudenko, E. V. and A. V. Sukhov, "Optically induced spatial charge separation in a nematic and the resultant orientational nonlinearity," *Journal of Experimental and Theoretical Physics*, Vol. 78, No. 6, 875–882, 1994.
59. Khoo, I. C., H. Li, and Y. Liang, "Observation of orientational photorefractive effects in nematic liquid crystals," *Optics Letters*, Vol. 19, 1723–1725, 1994.
60. Khoo, I. C., "Orientational photorefractive effects in nematic liquid crystal film," *IEEE J. Quant. Electronics*, Vol. 32, No. 3, 525–534, 1996.
61. Khoo, I. C., "Holographic grating formation in dye- and fullerene C_{60}-doped nematic liquid crystal film," *Optics Letters*, Vol. 20, 2137–2139, 1996.
62. Khoo, I. C., "Optical-DC-field induced space charge fields and photorefractive-like holographic grating formation in nematic liquid crystals," *Mol. Cryst. Liq. Cryst.*, Vol. 282, 53–66, 1996.
63. Khoo, I. C., S. Slussarenko, B. D. Guenther, and W. V. Wood, "Optically induced space charge fields, DC voltage, and extraordinarily large nonlinearity in dye-doped nematic liquid crystals,"

Optics Letters, Vol. 23, 253–255, 1998.

64. Lucchetti, L., M. Gentili, and F. Simoni, "Effects leading to colossal optical nonlinearity in dye-doped liquid crystals," *IEEE Journal of Selected Topics in Quantum Electronics*, Vol. 12, No. 3, 422–430, 2006.
65. Khoo, I. C., R. R. Michael, and P. Y. Yan, "Optically-induced molecular-reorientation in nematic liquid crystals and nonlinear optical processes in the nanosecond regime," *IEEE J. Quant. Electronics*, Vol. 23, No. 2, 267–272, 1987.
66. Khoo, I. C. and R. Normandin, "Nanosecond laser-induced transient and erasable permanent grating diffractions and ultrasonic waves in a smectic film," *J. Appl. Phys.*, Vol. 55, 1416–1418, 1984.
67. Khoo, I. C. and R. Normandin,"Nanosecond degenerate optical wave mixing and ultrasonic wave generation in the nematic phase of liquid crystals," *Optics Letters*, Vol. 9, 285–287, 1984.
68. Khoo, I. C., R. G. Lindquist, R. R. Michael, R. J. Mansfield, and P. Lopresti, "Dynamics of picosecond laser induced density, temperature and flow-reorientation effects in the mesophases of liquid crystals," *J. Appl. Phys.*, Vol. 69, 3853–3859, 1991.
69. Eichler, H. J. and R. Macdonald, "Flow alignment and inertial effects in picoseconds laser-induced reorientation phenomena of nematic liquid crystals," *Phys. Rev. Lett.*, Vol. 67, 2666–2669, 1991.
70. Khoo, I. C. and S. Shepard, "Submillisecond grating diffractions in nematic liquid crystal films," *J. Appl. Phys.*, Vol. 54, 5491–5493, 1983.
71. Hrozhyk, U. A., A. Uladzimir, S. V. Serak, N. V. Tabiryan, T. J. White, and T. J. Bunning, "Optically switchable, rapidly relaxing cholesteric liquid crystal reflectors," *Optics Express*, Vol. 18, 9651–9657, 2010.
72. White, T. J., R. L. Bricker, L. V. Natarajan, V. P. Tondiglia, L. Green, Q. Li, and T. J. Bunning, "Electrically switchable, photo-addressable cholesteric liquid crystal reflectors," *Optics Express*, Vol. 18, 173–178, 2010.
73. Khoo, I. C., J. H. Park, and J. D. Liou, "Theory and experimental studies of all-optical transmission switching in a twist-alignment dye-doped nematic liquid crystal," *J. Opt. Soc. Am. B*, Vol. 25, 1931–1937, 2008, and References therein.
74. Khoo, I. C., J. Liou, and M. V. Stinger, "Microseconds-nanoseconds all-optical switching of visible-near infrared, 0.5 μm–1.55 μm. Lasers with dye-doped nematic liquid crystals," *Mole. Cryst. Liq. Cryst.*, Vol. 527, 109–118, 2010.
75. Khoo, I. C., J. Liou, M. V. Stinger, and S. Zhao, "Ultrafast all-optical switching with transparent and absorptive nematic liquid crystals — implications in tunable metamaterials," *Mole. Cryst. Liq. Cryst.*, Vol. 543, 151–159, 2011.
76. Shishido, A., O. Tsutsumi, A. Kanazawa, T. Shiono, T. Ikeda, and N. Tamai, "Rapid optical switching by means of photoinduced change in refractive index of azobenzene liquid crystals detected by reflection-mode analysis," *J. Am. Chem. Soc.*, Vol. 119, 7791–7796, 1997.
77. Khoo, I. C., A. Diaz, S. Kubo, J. Liou, M. Stinger, T. Mallouk, and J. H. Park, "Nano-dispersed organic liquid and liquid crystals for all-time-scales optical switching and tunable negative- and zero-index materials," *Mole. Cryst. Liq. Cryst.*, Vol. 485, No. 1, 934–944, 2008.
78. Hwang, J., N. Y. Ha, H. J. Chang, B. Park, and J. W. Wu, "Enhanced optical nonlinearity near the photonic bandgap edges of a cholesteric liquid crystal," *Optics Letters*, Vol. 29, 2644, 2004.
79. Song, L., S. Fu, Y. Liu, J. Zhou, V. G. Chigrinov, and I. C. Khoo, "Direct femtosecond pulse compression with miniature-sized Bragg cholesteric liquid crystal," *Optics Letters*, Vol. 38, 5040–5042, 2013.
80. Khoo, I.C., S. Webster, S. Kubo, W. J. Youngblood, J. Liou, A. Diaz, T. E. Mallouk, P. Lin, D. Peceli, L. A. Padilha, D. J. Hagan, and E. W. Van Stryland, "Synthesis and characterization of the multi-photon absorption and excited-state properties of 4-propyl 4'-butyl diphenyl acetylene," *J. Mat. Chem.*, Vol. 19, 7525–7531, 2009.
81. Khoo, I. C. and A. Diaz, "Multiple-time-scales dynamical studies of nonlinear transmission of pulsed lasers in a multi-photon absorbing organic material," *J. Opt. Soc. Am. B*, Vol. 28, 1702–1710, 2011.

82. Khoo, I. C., A. Diaz, and J. Ding, "Nonlinear-absorbing fiber array for large dynamic range optical limiting application against intense short laser pulses," *J. Opt. Soc. Am. B*, Vol. 21, 1234–1240, 2004.
83. Khoo, I. C., A. Diaz, M. V. Wood, and P. H. Chen, "Passive optical limiting of picosecond-nanosecond lasers using highly nonlinear organic liquid cored fiber array," *IEEE Journal of Selected Topics in Quantum Electronics*, Vol. 7, No. 5, 760–768, 2001.
84. Khoo, I. C., "Nonlinear organic liquid cored fiber array for all-optical switching and sensor protection against short pulsed lasers," *IEEE Journal of Selected Topics in Quantum Electronics*, Vol. 14, No. 3, 946–951, 2008, and References therein.
85. He, G. S., L.-S. Tan, Q. Zheng, and P. N. Prasad, "Multiphoton absorbing materials: Molecular designs, characterizations, and applications," *Chemical Reviews*, Vol. 108, No. 3, 1245–1330, 2008, and References therein.
86. Takanashi, H., J. E. Maclennan, and N. A. Clark, "Sub 100 nanosecond pretilted planar-to-homeotropic reorientation of nematic liquid crystals under high electric field," *Jpn. J. Appl. Phys.*, Vol. 37, No. 5, 2587–2589, 1998.
87. Geis, M. W., R. J. Molnar, G. W. Turner, T. M. Lyszczarz, R. M. Osgood, and B. R. Kimball, "30 to 50 ns liquid-crystal optical switches," *Proc. SPIE*, Vol. 7618, 76180J/1–5, 2010.
88. Pawlik, G., K. Tarnowski, W. Walasik, A. C. Mitus, and I. C. Khoo, "Infrared cylindrical cloak in nanosphere dispersed liquid crystal metamaterial," *Optics Letters*, Vol. 37, 1847–1849, 2012.
89. Pawlik, G., G. Pawlik, W. Walasik, K. Tarnowski, A. C. Mitus, and I. C. Khoo, "Liquid crystal hyperbolic metamaterial for wide-angle negative-positive refraction and reflection," *Optics Letters*, Vol. 39, 1744–1747, 2014.
90. Jarema, M., W. Walasik, A. C. Mitus, and I. C. Khoo, "Field induced inhomogeneous index distribution of a nano-dispersed nematic liquid crystal near the Freedericksz transition: Monte carlo studies," *J. Opt. Soc. Am. B*, Vol. 27, No. 3, 567–576, 2010.
91. Pawlik, G., W. Walasik, A. C. Mitus, and I. C. Khoo, "Large gradients of refractive index in nanosphere dispersed liquid crystal metamaterial with inhomogeneous anchoring: Monte Carlo study," *Optical Materials*, Vol. 33, No. 9, 1459–1463, 2011.
92. Khoo, I. C. and T. H. Lin, "Nonlinear optical grating diffraction in dye-doped blue-phase liquid crystals," *Optics Letters*, Vol. 37, 3225–3227, 2012.
93. Chen, C.-W., H.-C. Jau, C.-T. Wang, C.-H. Lee, I. C. Khoo, and T.-H. Lin, "Random lasing in blue phase liquid crystals," *Optics Express*, Vol. 20, No. 21, 23978–23984, 2012.
94. Khoo, I. C., K. L. Hong, S. Zhao, D. Ma, and T.-H. Lin, "Blue-phase liquid crystal cored optical fiber array with photonic bandgaps and nonlinear transmission properties," *Optics Express*, Vol. 21, No. 4, 4319–4327, 2013.
95. Chen, C. W., H. C. Jau, C. H. Lee, C. C. Li, C. T. Hou, C. W. Wu, T. H. Lin, and I. C. Khoo, "Temperature dependence of refractive index in blue phase liquid crystals," *Optical Materials Express*, Vol. 3, No. 5, 527–532, 2013.
96. Kikuchi, H., M. Yokota, Y. Hiskado, H. Yang, and T. Kajiyama, "Polymer-stabilized liquid crystal blue phases," *Nat. Mater.*, Vol. 1, 64–68, 2002.
97. Coles, H. and M. N. Pivnenko, "Liquid crystal 'blue phases' with a wide temperature range," *Nature*, Vol. 436, 997–1000, 2005.
98. Hisakado, Y., H. Kikuchi, T. Nagamura, and T. Kajiyama, "Large electro-optic Kerr effect in polymer-stabilized liquid-crystalline blue phases," *Adv. Mater.*, Vol. 17, 96, 2005.
99. Ge, Z., S. Gauza, M. Jiao, H. Xianyu, and S.-T. Wu, "Electro-optics of polymer-stabilized blue phase liquid crystal displays," *Appl. Phys. Lett.*, Vol. 94, 101104, 2009.